

# Density-functional treatment of model Hamiltonians: basic concepts and application to the Heisenberg model\*

Valter L. Líbero and Klaus W. Capelle  
Departamento de Física e Informática  
Instituto de Física de São Carlos  
Universidade de São Paulo  
Caixa Postal 369, 13560-970 São Carlos, SP, Brazil

November 14, 2018

## Abstract

We describe how density-functional theory, well-known for its many uses in *ab initio* calculations of electronic structure, can be used to study the ground state of inhomogeneous model Hamiltonians. The basic ideas and concepts are discussed for the particular case of the Heisenberg model. As representative applications, illustrating scope and limitations of the procedure, we calculate the ground-state energy of one-, two- and three-dimensional antiferromagnetic Heisenberg models in the presence of boundaries and of impurities in the bulk and at the surfaces. Correlations are shown to lift degeneracies present in the mean-field approximation. Comparison with exact (brute force) diagonalization shows that the density-functional results are a significant improvement over the mean-field ones, at negligible extra computational cost.

---

\*This is the (slightly modified) English translation of a chapter, originally written in Portuguese, of a proceedings volume on density-functional theory: *40 anos DFT: Uma perspectiva Brasileira*, eds. K. Capelle, A. J. R. da Silva and A. Fazzio.

## Contents

1	Introduction	3
2	Comparison between <i>ab initio</i> DFT and DFT for model Hamiltonians	4
3	The Heisenberg model	5
4	Ground-state energy of the homogeneous Heisenberg model	7
5	Ground-state energy of the inhomogeneous Heisenberg model: spin-distribution functionals and local-spin approximation	8
6	Applications: Finite-size quantum spin chains, ladders and cubes	9
7	Summary	13
	References	14

## List of Tables

1	Diferent realizations of the concepts of DFT. . . . .	5
2	Ground-state energy $-E_0/NJ$ in the mean-field approximation, of a $4 \times 4 \times 4$ cube with 63 spin 1/2 sites and one impurity spin $S_I$ . . . . .	11
3	Ground-state energy $-E_0/NJ$ in the LSA <sup>SW</sup> , of a $4 \times 4 \times 4$ cube with 63 spin 1/2 sites and one imurity spin $S_I$ . . . . .	11

## List of Figures

1	Ground-state energy of an open 10-site chain of spin 1/2 atoms. . . . .	9
2	Ground-state energy of an $N_x \times N_y$ lattice of $S = 1/2$ spins. . . . .	10
3	$4 \times 4 \times 4$ cube of spin 1/2 with a substitutional impurity. . . . .	12

# 1 Introduction

Traditional density-functional theory (DFT) is based on the Hohenberg-Kohn theorem, according to which all observables of a quantum many-body system are determined uniquely by the ground-state charge density [1, 2]. These observables are thus functionals of the density, and a major task of DFT is the construction of ever better functionals for calculating, e.g., ground-state energies in terms of the ground-state density. The local-density approximation (LDA) is one such functional, expressing the exchange-correlation ( $xc$ ) energy of an inhomogeneous many-particle system in terms of its charge density. The density itself is normally calculated by means of a self-consistent field (SCF) procedure, solving effective single-particle equations known as the Kohn-Sham equations [3].

While widely used in electronic-structure calculations, both in solid-state physics and in quantum chemistry, the concepts and tools of DFT, such as the Hohenberg-Kohn theorem, the Kohn-Sham equations, and the LDA and its many improvements, are much more general, and can be applied to many quantum systems not described by the *ab initio* (Coulomb) Hamiltonian underlying applications of DFT in band-structure and quantum-chemical calculations.

In particular, they can also be applied to model Hamiltonians. In a model Hamiltonian description of a physical phenomenon one does not primarily focus on material-specific details, but on generic features of classes of systems. The use of such models has a long tradition in many-body physics and statistical mechanics, and the list of common models is long and includes famous examples such as the Ising, Heisenberg and Hubbard models.

DFT can be a useful tool in the study of such models in the presence of inhomogeneities [4, 5, 6]. Below we briefly describe the construction and some representative applications of DFT for the antiferromagnetic Heisenberg model [5, 7, 8]. To prepare the ground, we present in Sec. 2 a systematic comparison between traditional *ab initio* (Coulomb) DFT and DFT for model Hamiltonians. Section 3 introduces the Heisenberg model. In Sec. 4 we describe expressions for the ground-state and correlation energy of homogeneous (spatially uniform) Heisenberg models. In Sec. 5 we use these expressions, in the spirit of an LDA, to construct a local-spin approximation for inhomogeneous one, two and three-dimensional Heisenberg models. In Sec. 6 these functionals are used to calculate the ground-state energy of inhomogeneous chains, ladders and cubes, and compared with mean-field and exact diagonalization data. Sec. 7 contains a brief summary and assessment of the approach.

## 2 Comparison between *ab initio* DFT and DFT for model Hamiltonians

In Table 1 we present a schematic comparison between traditional, *ab initio*, DFT and DFT for two widely studied model Hamiltonians defined on lattices, the Hubbard and the Heisenberg model. The basic idea of lattice DFT for model Hamiltonians goes back to Gunnarsson and Schönhammer [9], in the context of the Hubbard model. A viable parametrization for the model's *xc* energy was proposed in [4], while corresponding work for the Heisenberg model is based on [5]. The following paragraphs describe Table 1, line by line.

Starting point is, in all cases, a Hohenberg-Kohn (HK) theorem, establishing that an intensive density-like quantity, coupled to a suitable generating field, determines the ground-state wave function of the model under study. While in *ab initio* DFT this intensive variable is the charge density  $n(\mathbf{r})$ , in lattice DFT for the Hubbard model it is the site occupation number  $n_i$ , and for the Heisenberg model it is the local spin  $\mathbf{S}_i$ .

Having proven a Hohenberg-Kohn theorem, the variational principle allows us to obtain the ground-state energy and the ground-state density distribution by minimizing a density functional. In *ab initio* (Coulomb) DFT and Hubbard DFT this minimization is normally done indirectly, via self-consistent solution of Kohn-Sham (KS) equations. This indirect minimization allows one to circumvent having to approximate the single-particle kinetic energy as a density functional. The Heisenberg model does not have a kinetic-energy term, and the minimization is most conveniently performed directly.

The *xc* energy is also unknown. Starting point for most approximation schemes for the *xc* functional is the local-density approximation, in which one first defines an auxiliary spatially uniform many-body problem, which can be solved more easily. In *ab initio* DFT this auxiliary many-body system is the *homogeneous* electron liquid, while for lattice DFTs spatial uniformity means equivalent sites. The solution of this uniform auxiliary problem may be very difficult, but it is still a lot simpler than the solution of the *inhomogeneous* many-body problem. In *ab initio* DFT the best values for the *xc* energy come from Quantum Monte Carlo simulations [10]. The one-dimensional Hubbard model, and the one-dimensional spin one-half Heisenberg model, have formally exact solutions by means of the Bethe Ansatz. For these systems the *xc* energy can be extracted, in principle, exactly. In higher dimensions or for larger spins this can only be done approximately.

Having solved the spatially uniform system, the usual next step is to parametrize the *xc* energy in a form convenient for numerical calculations. In *ab initio* calculations common parametrizations are those of Vosko, Wilk and Nusair (VWN) [11], Perdew and Zunger (PZ) [12], and Perdew and

Table 1: Different realizations of the concepts of DFT. See the main text for a description of the various entries.

	<b>Coulomb</b>	<b>Hubbard</b>	<b>Heisenberg</b>
HK	$\Psi[n(\mathbf{r})]$	$\Psi[n_i]$	$\Psi[\mathbf{S}_i]$
KS	SCF	SCF	————
homog. system	electron liquid	equivalent sites	equivalent sites
$e^{hom}$	QMC	BA	SW, BA, DMRG
parametrizations of $e^{hom}$ (LDA)	VVW, PZ, PW [11, 12, 13]	PRL <b>90</b> , 146402 (2003) [4]	PRB <b>68</b> , 024423 (2003) [5]
inhomog. system	inhomog. Coulomb systems	inhomog. Hubbard model	inhomog. Heisenberg model
applications	atoms, molecules solids ...	inequivalent sites, CDW, SDW, boundaries, impurities, external fields ...	

Wang (PW) [13]. For the Hubbard model a viable parametrization was proposed in [4]. Alternative approaches are discussed in [9, 14]. For the Heisenberg model several parametrizations were proposed in [5]. Some of these are briefly described below.

Once a parametrization of the per-site  $xc$  energy of the uniform model is available, it can be applied site by site in the corresponding inhomogeneous model. In *ab initio* calculations the inhomogeneity arises from the crystal lattice in a solid, or the atomic nuclei in a molecule. In lattice models it arises from inequivalent sites. For the Heisenberg model three examples of such lattice-DFT calculations for models with inequivalent sites are given below. These examples complement those presented in [7].

### 3 The Heisenberg model

One of the requirements on a formalism purporting to describe the magnetic properties of matter is that it should predict the existence of long-range order of ferro or antiferromagnetic nature [15, 16]. Within DFT, this requirement is met by spin-density-functional theory (SDFT). Within model Hamiltonians, the simplest model displaying such order is the Heisenberg model.

$$\hat{H} = \sum_{\langle ij \rangle} J_{ij} \hat{\mathbf{S}}_i \cdot \hat{\mathbf{S}}_j, \quad (1)$$

in which  $J_{ij}$  is the "exchange interaction" between spins at nearest-neighbour sites. The terminology "exchange" here arises from the original motivation for writing Eq. (1) as an effective model accounting for the consequences of the Pauli exclusion principle [17, 18]. However, if  $J_{ij}$  is calculated from many-body theory or fitted to experiment, it generally also contains contributions from correlation, i.e., many-body effects beyond the single-determinant (Hartree-Fock like) approximation.

Depending on the sign of  $J_{ij}$  and its dependence on the site labels  $i$  and  $j$ , the model (1) can have ferromagnetic, antiferromagnetic or noncollinear spin configurations [16]. Below we focus on the antiferromagnetic case, which is relevant for a large class of magnetic insulators, among which the undoped state of cuprate superconductors may be one of the most important [19]. However, the applications of model (1) transcend the boundaries of physics, as illustrated by chemical applications to the magnetic states of conjugated hydrocarbons and organometallic compounds [19-24].

Although almost 80 years have passed since the model (1) was first proposed, a complete solution is known only for the limiting cases of few sites and, by means of the Bethe Ansatz (BA), for spin  $S = 1/2$  in one dimension [26, 27]. Complete numerical diagonalization is possible for up to a few dozens of sites. The density-matrix renormalization group (DMRG) and Quantum Monte Carlo (QMC) techniques can be applied also to larger systems, but at considerable computational cost.

Moreover, all these techniques, BA, DMRG, QMC, etc. encounter significant difficulties in spatially nonuniform systems, with broken translational symmetry, such as in the presence of impurities, boundaries or externally applied nonuniform fields. A modification of the homogeneous Heisenberg model describing this type of inhomogeneity is

$$\hat{H} = \sum_{ij} J_{ij} \hat{\mathbf{S}}_i \cdot \hat{\mathbf{S}}_j + \sum_i \hat{\mathbf{S}}_i \mathbf{B}_i, \quad (2)$$

where  $\mathbf{B}_i$  is an external or internal magnetic field, which can vary from one site to the next, and  $J_{ij}$  extends the spin-spin coupling to other than nearest neighbours.

In these situations DFT provides a computationally viable approach to the ground-state energy and density, and their dependence on the system parameters. However, as explained in the preceding section, already the simplest practical approximation to DFT, the LDA, requires as an input the solution of the uniform system. For this reason we turn, in the next section, to a brief discussion of the ground state and correlation energy of the homogeneous Heisenberg model.

## 4 Ground-state energy of the homogeneous Heisenberg model

The simplest approximation to Hamiltonian (1) is the mean-field (MF) one, in which the vector operators  $\hat{\mathbf{S}}$  are substituted by classical (commuting) vectors  $\mathbf{S}$ . In this approximation the per-spin ground-state energy of a homogeneous linear, quadratic or cubic lattice comprising  $N$  sites with spin  $S$ , in  $d$  dimensions, is

$$e_0^{MF}(S) \equiv \frac{E_0^{MF}(S)}{N} = -Jd S^2. \quad (3)$$

An improved estimate of this energy can be obtained from spin-wave (SW) theory [28], according to which

$$e_0^{SW}(S) = -Jd S^2 + Jd^{-1/5} \left( \frac{2}{\pi} - 1 \right) S = e_0^{MF}(S) + Jd^{-1/5} \left( \frac{2}{\pi} - 1 \right) S. \quad (4)$$

(Here we have used the conjecture of Ref. [5] to write the last term as a closed function of  $d$ .) As an example, for  $d = 1$  and  $S = 1/2$ , spin-wave theory predicts  $e_0^{SW} = -0.431690J$ , which is about 2.6% off the exact Bethe-Ansatz result  $e_0^{BA} = (1/4 - \ln 2)J$ .

The correlation energy  $e_c(S)$  is defined as the difference  $e_0(S) - e_0^{MF}(S)$ , where  $e_0(S)$  is the exact ground-state energy. Within SW theory, we have thus

$$e_c^{SW}(S) = e_0^{SW}(S) - e_0^{MF}(S) = Jd^{-1/5} \left( \frac{2}{\pi} - 1 \right) S. \quad (5)$$

A more precise expression for  $e_c(S)$  in  $d = 1$  has recently been proposed [5, 29] on the basis of previously obtained density-matrix renormalization group data [29],<sup>1</sup>

$$\begin{aligned} \frac{e_c^{DMRG}(S)}{J} &= \frac{e_c^{SW}(S)}{J} - 0.03262 - \frac{0.0030}{S} + \frac{0.0015}{S^3} \\ &\quad - \left( 0.338 - \frac{0.28}{S} + \frac{0.035}{S^3} \right) e^{-\pi S} \cos(2\pi S). \end{aligned} \quad (6)$$

For  $S = 1/2$  this expression predicts  $e_0^{DMRG} = -0.446253J$ , which deviates only by 0.7% from the exact result.

The utility of the MF, SW and DMRG expressions for  $e_0(S)$  is, *a priori*, rather limited: MF theory is not reliable due to its neglect of correlation, and the SW and DMRG expressions are only applicable to spatially uniform systems, in which  $S$  is a constant. (The DMRG expression is also limited to  $d = 1$ .) Restriction to spatial homogeneity is a serious limitation, since

<sup>1</sup>The fit originally proposed in Ref. [29] did not include the cubic terms in  $1/S$  and did not recover the Bethe-Ansatz exact result at  $S = 1/2$ . The cubic terms were added in Ref. [5] in order to extend the fit to  $S = 1/2$ .

spatial inhomogeneities are ubiquitous in real systems. Examples are effects of external magnetic fields, magneto-crystalline anisotropy, boundaries, impurities, defects etc. Such situations are hard to deal with by traditional methods because translational symmetry is broken. To overcome this difficulty we employ density-functional theory [2, 30], within which expressions for the uniform system find applications as input for LDA-type approximations for inhomogeneous systems.

## 5 Ground-state energy of the inhomogeneous Heisenberg model: spin-distribution functionals and local-spin approximation

The Hohenberg-Kohn theorem for the Heisenberg model, proved in Ref. [5], shows that the expectation value of any observable  $\hat{O}$  of that model is a functional of the ground-state spin distribution  $\mathbf{S}_i$ , given, in principle, as  $O[\mathbf{S}_i] = \langle \Psi[\mathbf{S}_i] | \hat{O} | \Psi[\mathbf{S}_i] \rangle$ , where  $\mathbf{S}_i = \langle \Psi | \hat{\mathbf{S}}_i | \Psi \rangle$  is a classical spin vector and not an operator. This functional is universal with respect to external fields  $\mathbf{B}_i$ , but not with respect to changes in the spin-spin interaction  $J_{ij}$ .

For the Heisenberg model the ground-state energy and its minimizing spin distribution are obtained most conveniently by direct minimization of the functional

$$E_0[\mathbf{S}_i] \equiv E_0^{MF}[\mathbf{S}_i] + E_c[\mathbf{S}_i]. \quad (7)$$

Here the mean-field term is a simple functional of  $\mathbf{S}_i$ ,

$$E_0^{MF}[\mathbf{S}_i] = J \sum_{\langle ij \rangle} \mathbf{S}_i \cdot \mathbf{S}_j, \quad (8)$$

which for homogeneous antiferromagnetic systems on linear, square and cubic lattices reduces to Eq. (3). To approximate  $E_c[\mathbf{S}_i]$  we employ the LDA concept, applied directly to the spin vectors. The resulting local-spin approximation (LSA) consists in substituting, locally, the variable  $S$  in the expressions for the homogeneous system, by the variable  $|\mathbf{S}_i|$ , according to

$$E_c[\mathbf{S}_i] \approx E_c^{LSA}[\mathbf{S}_i] = \sum_i \frac{E_c(S)}{N} |_{S \rightarrow |\mathbf{S}_i|} =: \sum_i e_c(S) |_{S \rightarrow |\mathbf{S}_i|}. \quad (9)$$

Within the SW approximation for  $E_c$  we thus have

$$E_c^{LSA-SW}[\mathbf{S}_i] = J d^{-1/5} \left( \frac{2}{\pi} - 1 \right) \sum_i |\mathbf{S}_i|, \quad (10)$$

so that the ground-state energy functional in the LSA<sup>SW</sup> becomes

$$E_0^{LSA-SW}[\mathbf{S}_i] = J \sum_{\langle ij \rangle} \mathbf{S}_i \cdot \mathbf{S}_j + J d^{-1/5} \left( \frac{2}{\pi} - 1 \right) \sum_i |\mathbf{S}_i|. \quad (11)$$



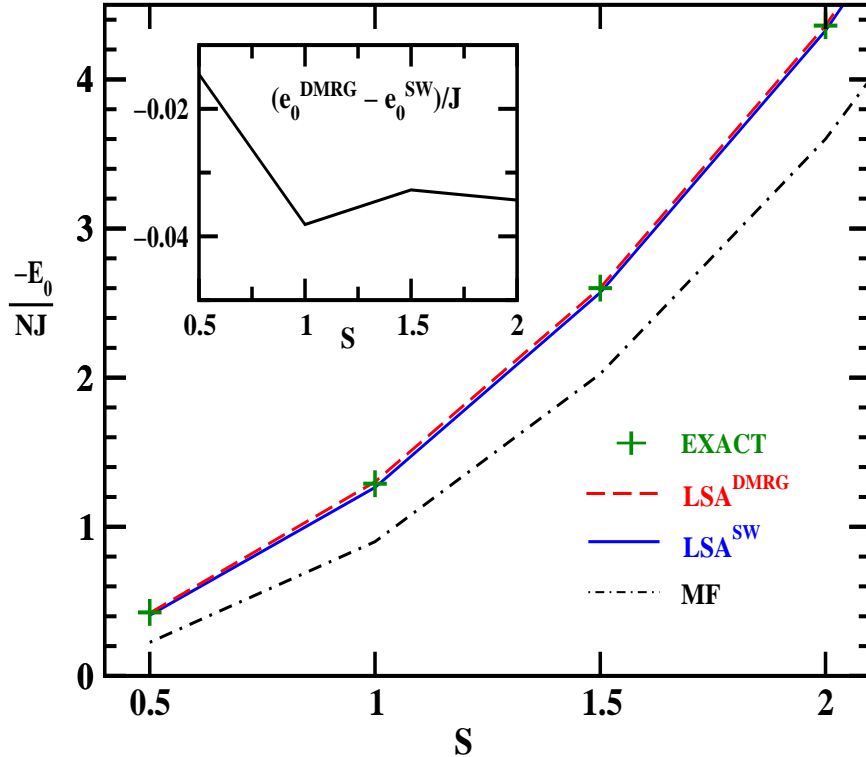


Figure 1: Per-site ground-state energy of an open 10-site chain of spin 1/2 atoms, obtained exactly, in the mean-field approximation, and with LSA. The inset illustrates the difference between  $LSA^{DMRG}$  and  $LSA^{SW}$ .

Similarly, the  $LSA^{DMRG}$  is

$$E_0^{LSA-DMRG}[\mathbf{S}_i] = J \sum_{\langle ij \rangle} \mathbf{S}_i \cdot \mathbf{S}_j + \sum_{\langle ij \rangle} e_c^{DMRG}(S) |_{S \rightarrow |\mathbf{S}_i|}, \quad (12)$$

where  $e_c^{DMRG}(S)$  is defined in Eq. (6).

## 6 Applications: Finite-size quantum spin chains, ladders and cubes

As an application of these approximations we now consider 10 spin  $S$  sites on a chain with open boundary conditions. As a consequence of the boundaries this is already an inhomogeneous system, in which not all sites are equivalent. In Fig. 1 we compare values for the per-site ground-state energy obtained from the mean-field approximation, with values obtained from the  $LSA^{SW}$  and  $LSA^{DMRG}$  functionals, for some values of the spin  $S$ . We also include exact values obtained from numerical diagonalization of Hamiltonian (1). The comparison of the three approximation schemes with the exact

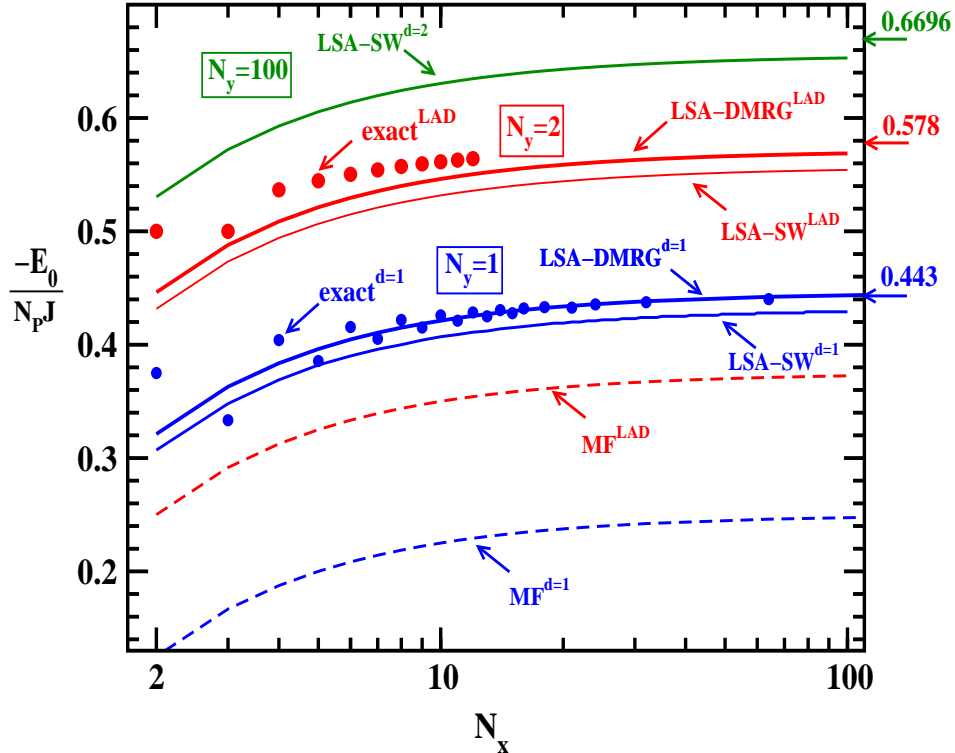


Figure 2: Per-site ground-state energy of an  $N_y \times N_x$  lattice of  $S = 1/2$  spins, with open boundary conditions.  $N_p = N_y \times N_x$  is the total number of sites, ranging from 2 to  $10^4$ . Curves and data pertaining to a one-dimensional chain of length  $N_x$  are in blue, those pertaining to two-legged ladders of size  $2 \times N_x$  in red, and the curve for multi-legged ladders of size  $100 \times N_x$  is in green. See main text for more detailed explanation of the different data sets and curves.

data illustrates the significant improvement obtained by means of the LSA, as compared to the MF approximation. It also illustrates that the  $\text{LSA}^{SW}$  and  $\text{LSA}^{DMRG}$  are very similar on this scale. In the inset we plot the difference  $e_0^{DMRG} - e_0^{SW}$  versus  $S$ , to illustrate the scale of the difference between both formulations of the LSA. For larger systems than  $L = 10$ , and/or larger spins than  $S = 2$ , full numerical diagonalization becomes computationally very expensive. On the other hand, cheap mean-field calculations are not reliable. The LSA concept is thus a useful tool for estimating energies of systems that are too large for exact calculations, at much better accuracy than obtained from mean-field calculations.

The main utility of the LSA concept, however, lies in the ease with which it is extended to higher dimensions or to more inhomogeneous systems. As a second illustrative application of the LSA we thus present, in Fig. 2, results

Table 2: Ground-state energy  $-E_0/NJ$  in the mean-field approximation, of a  $4 \times 4 \times 4$  cube with 63 spin  $1/2$  sites and one spin  $S_I$  site located on a corner, an edge, a face or in the bulk.

	1/2	1	3/2	2	5/2	3
corner	0.5625	0.5742	<b>0.5859</b>	0.5977	<b>0.6094</b>	<b>0.6211</b>
edge	0.5625	0.5781	0.5938	<b>0.6094</b>	0.6250	0.6406
face	0.5625	0.5820	0.6016	<b>0.6211</b>	0.6494	0.6602
bulk	0.5625	<b>0.5859</b>	<b>0.6094</b>	0.6328	0.6562	0.6797

Table 3: Ground-state energy  $-E_0/NJ$  in the LSA<sup>SW</sup> of the same system described in Table 2 and Fig. 3. Inclusion of correlation lifts the degeneracies predicted by the mean-field approximation.

	1/2	1	3/2	2	5/2	3
corner	0.7080	0.7220	<b>0.7360</b>	0.7500	<b>0.7640</b>	<b>0.7780</b>
edge	0.7080	0.7259	0.7438	<b>0.7617</b>	0.7796	0.7975
face	0.7080	0.7298	0.7516	<b>0.7734</b>	0.7952	0.8170
bulk	0.7080	<b>0.7337</b>	<b>0.7594</b>	0.7851	0.8108	0.8366

for systems representative of the crossover from one to two dimensions, such as spin ladders. Figure 2 contains two sets of exact data. The first, labelled  $\text{exact}^{d=1}$ , is the per-site energy of a linear open chain with  $N_x$  sites. For this same system we also show results from the mean-field approximation, Eq. (8) (labelled  $\text{MF}^{d=1}$ ), and the LSA<sup>DMRG</sup> and LSA<sup>SW</sup> approaches (labelled LSA-DMRG<sup>d=1</sup> and LSA-SW<sup>d=1</sup>, respectively). The arrow labelled 0.443 indicates the exact value in the thermodynamic limit  $N_x \rightarrow \infty$ , obtained from the Bethe-Ansatz. Comparing these data we see that the MF approximation fails badly, while LSA<sup>DMRG</sup> provides an excellent approximation to the exact data for not too small  $N$ .

The second set of exact data in Fig. 2, labelled  $\text{exact}^{LAD}$ , represents the energy of spin ladders of size  $2 \times N_x$ , as a function of  $N_x$ . Again, we compare the exact data with results from the mean field ( $\text{MF}^{LAD}$ ) and both local-spin (LSA-DMRG<sup>LAD</sup> and LSA-SW<sup>d=1</sup>) approximations. The arrow at 0.578 is the value extrapolated for  $N_x \rightarrow \infty$  from Quantum Monte Carlo data [31]. Although for the ladders LSA<sup>DMRG</sup> and LSA<sup>SW</sup> are not as good as for chains (which is easy to understand, considering the origin of their correlation energy in a one-dimensional system), it is still a significant improvement on the mean-field approximation, which for the two-legged ladder predicts energy values that fall closer to the exact ones for the chain than to those for the ladder itself. In numbers, at  $N_x = 12$  the MF approximation differs by 37% from the exact value, while the LSA<sup>DMRG</sup> value is

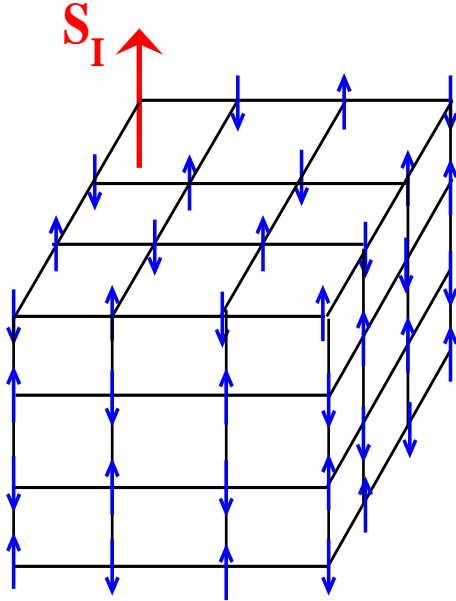


Figure 3:  $4 \times 4 \times 4$  cube of spin  $1/2$  with a substitutional impurity at the corner (illustrated), edge, face or in the bulk. The mean-field ground-state energies resulting from the different impurity positions show certain degeneracies that are lifted by inclusion of correlations. (See data in Table 2 and 3 and discussion in main text.)

off by 2.4%. Still in Fig. 2, the curve labelled LSA-SW $^{d=2}$  represents values for more and more two-dimensional systems, of size  $N_x \times 100$ , obtained by combining the two-dimensional mean-field approximation with the two-dimensional SW approximation as an input for LSA. The value obtained from LSA $^{SW}$  at  $N_x = 100$  deviates by only 3.2% from the asymptotic result  $0.6696J$ , estimated in Ref. [32].

As our third example we consider a three-dimensional cubic arrangement of spins with  $4 \times 4 \times 4 = 64$  spin  $1/2$  sites, one of which is replaced by a substitutional impurity of spin  $S_I$ . This impurity can sit in the bulk of the cube (8 equivalent positions), on one of its faces (24 equivalent positions), on an edge (24 equivalent positions), or on the corner sites (8 equivalent positions). Fig. 3 illustrates this system, and Tables 2 and 3 contain the corresponding mean-field and LSA $^{SW}$  ground-state energies for several values of  $S_I$ . We note that the mean-field approximation predicts certain degeneracies that are lifted on including correlation via the LSA: in the MF approximation an  $S_I = 2$  impurity on a face of the cube and an  $S_I = 3$  on a corner site are degenerate (both having energy  $e_0^{MF} = -0.6211J$ ), as are  $S_I = 1$  impurity in the bulk and an  $S_I = 3/2$  one at a corner ( $e_0^{MF} = -0.5859J$ ). A triple degeneracy occurs between an  $S_I = 5/2$  impurity at a corner, an  $S_I = 2$  one

on an edge site, and a  $S_I = 3/2$  one in the bulk. ( $e_0^{MF} = -0.6094J$ ). All of these degeneracies are lifted by correlations, which shows that they are artifacts of the mean-field approximation. This type of information could be useful for the design of self-assembled magnetic nanostructures, in which the magnetic atoms will tend to spontaneously occupy the energetically favoured sites. Other applications of the LSA<sup>SW</sup> and LSA<sup>DMRG</sup> functionals can be found in Refs. [5, 7, 8].

## 7 Summary

The above examples show that DFT within the local-spin approximation can be a useful tool for calculating ground-state energies of spatially inhomogeneous Heisenberg models. The computational effort is much less than for a QMC or DMRG calculation, allowing applications to systems in two or three dimensions, and with reduced translational symmetry.

Exact or nearly exact benchmark values can only be obtained for small numbers of sites and simple geometries, or in the thermodynamic limit. LSA calculations, on the other hand, are not more expensive, computationally, than the mean-field ones, and much more accurate, but this advantage is partially offset by the fact that, unlike an exact, BA, or QMC calculation, LSA does not yield the many-body wave function. LSA is also less accurate than DMRG, but more easily applicable to systems in two and three dimensions.

Methodologically, DFT for the Heisenberg model differs in three aspects from Coulomb (*ab initio*) DFT [2] and from DFT for the Hubbard model [4]: (i) LSA proceeds exclusively in terms of the spin density and makes no use of the charge density (differently from the local-spin-density approximation of Coulomb DFT, which uses charge and spin densities). (ii) Numerical results are obtained by directly minimizing an energy functional, and not via self-consistent solution of effective single-particle equations. In this sense Heisenberg-model DFT in the LSA represents a realization of orbital-free-DFT [33]. (iii) For the Heisenberg model the dependence of the correlation functional on dimensionality is known to a good approximation [5]. This dependence is unknown in other formulations of DFT.

This last observation also represents a different way in which DFT for model Hamiltonians can be useful: While the above mostly focused on how DFT can be usefully employed to obtain information on model Hamiltonians, it is also possible to regard these models as theoretical laboratories in which concepts and tools of DFT can be investigated in a simpler and better controlled environment than in an *ab initio* calculation.

*Acknowledgements:* This work was supported by FAPESP and CNPq. We thank F. C. Alcaraz and L. N. Oliveira for useful discussions on the Bethe Ansatz and the Heisenberg model.

## References

- [1] P. Hohenberg and W. Kohn, Phys. Rev. **136**, B864 (1964).
- [2] W. Kohn, Rev. Mod. Phys. **71**, 1253 (1999).
- [3] W. Kohn and L. J. Sham, Phys. Rev. **140**, A1133 (1965).
- [4] N. A. Lima, M. F. Silva, L. N. Oliveira and K. Capelle, Phys. Rev. Lett **90**, 146402 (2003).
- [5] V. L. Líbero and K. Capelle, Phys. Rev. B **68**, 024423 (2003).
- [6] R. J. Magyar and K. Burke, Phys. Rev. A **70**, 032508 (2004).
- [7] P. E. G. Assis, Valter L. Líbero and K. Capelle, Phys. Rev. B **71**, 052402 (2005).
- [8] K. Capelle and Valter L. Líbero, Int. J. Quantum Chem., accepted (2005). Also available as cond-mat/0506167.
- [9] O. Gunnarsson and K. Schönhammer, Phys. Rev. Lett. **56**, 1968 (1986).  
K. Schönhammer, O. Gunnarsson, and R. M. Noack, Phys. Rev. B **52**, 2504 (1995).
- [10] D. M. Ceperley and B. J. Alder, Phys. Rev. Lett. **45**, 566 (1980).
- [11] S. H. Vosko, L. Wilk, and M. Nusair, Can. J. Phys. **58**, 1200 (1980).
- [12] J. P. Perdew and A. Zunger, Phys. Rev. B **23**, 5048 (1981).
- [13] J. P. Perdew and Y. Wang, Phys. Rev. B **45**, 13244 (1993).
- [14] R. López-Sandoval and G. M. Pastor, Phys. Rev. B **67**, 035115 (2003).
- [15] H. E. Stanley, *Introduction to Phase Transitions and Critical Phenomena* (Oxford University Press, Oxford, 1971).
- [16] J. S. Smart, *Effective Field Theories of Magnetism* (W. B. Saunders Company, Philadelphia, 1966).
- [17] W. Heisenberg, Z. Phys. **38**, 441 (1926), Z. Phys. **49**, 619 (1928).
- [18] P. A. M. Dirac, Proc. Roy. Soc. **112A**, 661 (1926), Proc. Roy. Soc. **123A**, 714 (1929).
- [19] E. Manousakis, Rev. Mod. Phys. **63**, 1 (1991).
- [20] N. Guihery, N. Ben Amor, D. Maynau and J. P. Malrieu, J. Chem. Phys. **104**, 3701 (1996).

- [21] M. Said, D. Maynau, J. P. Malrieu and M. A. Garcia Bach, *J. Am. Chem. Soc.* **106**, 571 (1984).
- [22] A. L. Tchougreeff, *J. Chem. Phys.* **96**, 6026 (1992).
- [23] C. Kollmar and O. Kahn, *J. Chem. Phys.* **98**, 453 (1993).
- [24] M. Matusiewicz, M. Czerwinski, J. Kasperczyk and I. V. Kityk, *J. Chem. Phys.* **111**, 6446 (1999).
- [25] J. H. Luscombe, M. Luban and F. Borsa, *J. Chem. Phys.* **108**, 7266 (1998).
- [26] H. Bethe, *Z. Phys.* **71**, 205 (1931).
- [27] L. Hulthen, *Arkiv Mat. Astron. Fysik* **26A**, No.11, 1 (1938).
- [28] P. W. Anderson, *Phys.Rev.* **86**, 694 (1952).
- [29] J. Lou, S. Qin, T.-K. Ng and Z. Su, *Phys. Rev. B* **65**, 104401 (2002).
- [30] R. M. Dreizler and E. K. U. Gross, *Density Functional Theory* (Springer, Berlin, 1990).
- [31] T. Barnes, E. Dagotto, J. Riera and E. S. Swanson, *Phys. Rev. B* **47**, 3196 (1998).
- [32] S. Liang, *Phys. Rev. B* **42**, 6555 (1990).
- [33] B. J. Zhou, V. L. Ligneres and E. A. Carter, *J. Chem. Phys.* **122**, 044103 (2005).